INFLUENCE OF OPERATING CONDITIONS ON AMMONIUM BISULFATE DEPOSITION IN THE ROTARY AIR PREHEATER OF COAL-FIRED POWER PLANTS

by

Limin WANG[a], Yufan BU[a], Yang HE[a], Chunli TANG[b], Lei DENG[a], and Defu CHE[a*]

[a] State Key Laboratory of Multiphase Flow in Power Engineering, Xi'an Jiaotong University, Xi'an, China
[b] School of Human Settlements and Civil Engineering, Xi'an Jiaotong University, Xi'an, China

Original scientific paper
https://doi.org/10.2298/TSCI180524213W

To achieve the maximum NO_x reduction in coal-fired power plant, excess ammonia is injected into the selective catalytic reduction reactor, which leads to the formation of ammonium bisulfate due to the reaction between ammonia escaping from the selective catalytic reduction reactor and SO_x in the flue gas. Ammonium bisulfate can condense in the rotary regenerative air-preheater, which would adversely affect the safe and efficient operation of the air-preheater. An improved radian number is proposed to estimate the ammonium bisulfate deposition. The operating conditions or modes of the air-preheater, i. e., air-flow bypass, cold-end protection and different splitting fluid sector arrangements, are comparatively studied to analyze the temperature and ammonium bisulfate deposition distributions. The hot air re-circulation is not helpful to mitigate the ammonium bisulfate deposition in medium matrix layer. The splitting gas sector arrangement would cause more serious plugging problem, but the splitting air sector arrangements can alleviate the ammonium bisulfate deposition. To increase the air bypass rate is more effective than the splitting air sector arrangements to alleviate the plugging problem. The improved radian number is more reasonable to reflect the ammonium bisulfate deposition compared with the original radian number.

Key words: *rotary regenerative air-preheater, operating condition, ammonium bisulfate deposition, improved radian number*

Introduction

Environmental protection has been given more and more attention due to the serious impacts of environmental problems on human health and economic development. The updated regulations have been issued to give more stringent contaminant emission standards for NO_x, SO_x and particulate matter to push coal-fired power plant to achieve the ultra-low air pollutant emission [1, 2].

The selective catalytic reduction (SCR) technology has been extensively used in Chinese coal-fired power plants to realize the lower NO_x emission [3]. To achieve the maximum NO_x reduction, excess ammonia is generally injected into the SCR reactor, so there is an

* Corresponding author, e-mail: dfche@mail.xjtu.edu.cn; dfche.xjtu@gmail.com

inevitable ammonia slip at the outlet of the SCR reactor. Ammonia escaped from the SCR reactor can react with SO_x and water vapor in the flue gas to form ammonium sulfate (AS) and bisulfate (ABS) in the downstream flue gas [4]. The ABS has a higher dew point and can condense in the middle and cold layers of rotary regenerative air-preheater (RAPH). Liquid ABS can capture fly ash and other complex particles in the flue gas such as sulfuric acid droplets, ammonium nitrate, and calcium salt and finally lead to the plugging and corrosion of RAPH [1, 5-7]. The plugging can increase the pressure drop in the RAPH and then reduce the unit load due to the limit of induced draft fan [1]. The corrosion would reduce the heat transfer efficiency and shorten the life of the heat transfer elements of RAPH. The plugging and corrosion caused by ABS deposition have become urgent problems for RAPH. The ABS deposition is directly related to the local temperature of the matrix. Besides, the ABS deposition in the cold layer zone is easier to clean than that in the middle layer because the penetration of soot blowing device would decay dramatically through the gap between cold and middle layers. Therefore, the evaluation of the location of ABS deposition is quite important during the design process of RAPH.

Numerous studies have been conducted on the formation mechanism of ABS, and various approaches have been proposed to reduce the impacts of ABS deposition on RAPH. Burke and Johnson [5] conducted a kinetic analysis of the NH_3-SO_3 reactions and found that both AS and ABS could form in the middle and cold layers of an RAPH. They found that ABS was the first compound formed under the time temperature histories in an RAPH and the reaction which forms ABS from gaseous reactants was more rapid than the reaction which forms AS. A kinetic equation for ABS formation in the RAPH was proposed by Radian in 1982 to characterize the ABS formation rate [8]. The radian number was first proposed to model the foreseeable blockage status of RAPH using feasible measuring parameters. Chothani *et al.* [9] measured the formation temperature and evaporation temperature of ABS by using the measurement sensor. Based on the measurement, the condensation of ABS was predicted by using an online air heater thermodynamic model. Si *et al.* [10] carried out field tests to study the variation of ABS formation temperature at a coal-fired power plant by using an on-line ABS probe, and proposed two inferential sensor models to infer ABS formation temperature based on real process variables and predict value from the input variables, respectively. Menasha *et al.* [6] investigated the formation temperature and deposition characteristics of ABS by experimental simulation and found that the ABS formation temperature lies in the range of 500-520 K for typical flue gas concentrations of ammonia and SO_x species. However, there is still not a number that can estimate the ABS condensation status in the RAPH during the design process.

Vuthaluru *et al.* [1] used a combination of ash chemistry and quantitative X-ray diffraction analysis to examine the deposit samples collected in the selected regions of RAPH. They indicated that the large temperature fluctuation of the RAPH is a significant factor for deposition formation. Therefore, the operating conditions or modes of RAPH can influence the ABS deposition since it can greatly change the temperature distribution of rotor. In application, operators try to change the temperature distribution on the rotor of RAPH to prevent cold end corrosion induced by sulfuric acid in flue gas by changing operating conditions. For example, the cold end protection by steam-air heater or hot air re-circulation is extensively used to control the average cold end temperature of RAPH. Most investigations focused on the effects of different operation modes on the efficiency and the average cold end temperature of RAPH. However, few researchers have studied the influence of operating conditions on the characteristic of ABS deposition area in RAPH.

The main purpose of this paper is to propose an improved radian number which could be used to evaluate the ABS deposition status in the design process of RAPH and then comparatively analyze the effects of different operation conditions and modes, *i. e.* cold end protection, air-flow bypass and splitting fluid sector arrangements, on the ABS deposition distribution in RAPH.

The RAPH and operating conditions investigated

The RAPH parameters

Figure 1 shows the 3-D structure schematic and 2-D rotor schematic of a tri-sector RAPH used in a 600 MW coal-fired power plant in China, which consists of three matrix-layers and three fluid sectors. The three-layers include a hot-layer, a middle-layer and a cold-layer in axial direction. The fluid sectors consist of gas-, secondary-air- and primary-air sectors of 180°, 120° and 60°, respectively. Table 1 presented the detailed parameters of this RAPH, including the type, rotor diameter, diameter, rotor speed, and the fluid-flow rate and inlet temperature of each sector. The heat transfer element, HE1, is used in the hot- and middle-layers, and the HE2 is used in the cold-layer. Table 2 shows the physical parameters including plate thickness, density, thermal conductivity, specific heat, heat transfer area density, the fraction of solid, hydraulic diameter, and heat transfer co-relations of these two kinds of heat transfer elements. The heat transfer co-relations are achieved by series of experiments by a manufacturer of China.

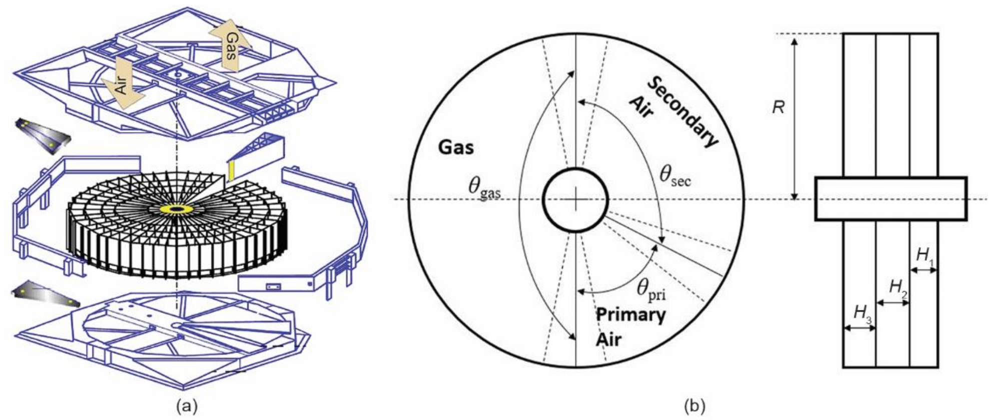

Figure 1. The 3-D structure schematic (a) and 2-D rotor schematic (b) of a tri-sector air-preheater

Table 1. Geometrical and operational parameters of the air preheater

Parameters	R_{rotor} [m]	R_{center} [m]	H_1+H_2 [mm]	H_3 [mm]	Ω [rmin^{-1}]	$\dot{m}_g$ [kgh^{-1}]	$\dot{m}_{pri}$ [kgh^{-1}]	$\dot{m}_{sec}$ [kgh^{-1}]	$T_{g,in}$ [°C]	$T_{pri,in}$ [°C]	$T_{sec,in}$ [°C]
Value	8.211	1.626	1600	900	1.0	2774369	965253	1629116	397	20	20

Table 2. Parameters of two kinds of heat transfer elements

Parameters	δ [mm]	ρ [kgm^{-3}]	λ [Wm^{-1}K^{-1}]	C [Jkg^{-1}K^{-1}]	β [m^{2}m^{-3}]	φ [–]	D_h [m]	Heat transfer correlation
HE1	0.5	753.35	52.92	456	420.21	0.096	0.0086	Nu = 0.083 Re$^{0.69}$Pr$^{0.4}$
HE2	1	1234.22	52.92	456	344.23	0.157	0.0098	Nu = 1.112 Re$^{0.64}$Pr$^{0.4}$

Cold-end protection

To protect the cold layer matrix from low temperature induced by sulfuric acid in the flue gas, cold-end protection, *i. e.*, hot air re-circulation and inlet air heater, are used to increase the average cold end temperature in application. However, the effects of hot air re-circulation and inlet air heater on ABS deposition in RAPH is still not reported. The effects of different re-circulation rates of primary air and secondary air on ABS deposition are investigated in this paper. The re-circulation rate is defined as $X_r = \dot{m}_r/\dot{m}_0$, where $\dot{m}_r$ and $\dot{m}_0$ represent the re-circulation mass-flow rate and the total mass-flow rate, respectively.

In the inlet air heater mode, the air is heated before entering the RAPH by the steam extracted from turbines. The influence of different air inlet temperature on the ABS deposition is investigated.

Air-flow bypass

To decrease the influence of plugging induced by ABS deposition, a portion of the air-flow is bypassed to increase the average temperature of the matrix in the rotor [9]. The primary air bypass is more commonly used to control the temperature of hot primary air at the outlet of RAPH, since the hot primary air should not be too hot to pass through the warehouse of pulverized coal. Thus, the primary air bypass cannot be used to ensure the safety of coal feeding and alleviate the plugging, simultaneously. So, this paper will discuss the effect of secondary air bypass on ABS deposition. The bypass rate is defined as $X_b = \dot{m}_b/\dot{m}_0$, where $\dot{m}_b$ represents the bypass mass-flow rate.

Splitting flow arrangement

In application, the hot gas and cold air are commonly in a countercurrent arrangement in order to obtain higher efficiency, which leading to a larger temperature difference between the hot and cold ends. In order to decrease the temperature difference and improve the whole average temperature, this paper proposes a kind of splitting design, in which a fluid sector is split into two sub-sectors and the fluid in one sub-sector (named sector-A) keeps the original flow direction while the fluid in the other sub-sector (named sector-B) flows in the counter direction. Though this splitting flow arrangement would reduce the efficiency, it could change the temperature profile along axial direction of RAPH and help to solve the plugging and corrosion problem induced by ABS deposition. This paper will investigate the temperature and ABS deposit distributions in the RAPH under different splitting flow design conditions, namely splitting gas sector design, splitting secondary air sector design and splitting primary air sector design, as shown in fig. 2. In each arrangement, the splitting ratio, $X_c = \dot{m}_c/\dot{m}_0$, is defined as the ratio between the flow rate in the counter direction and total orig-

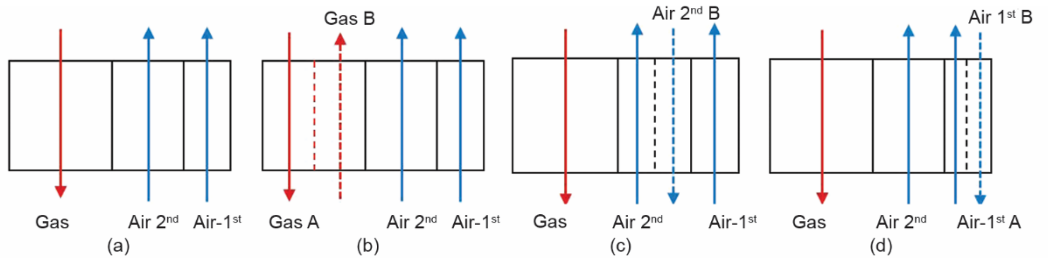

Figure 2. Splitting fluid sector arrangements in whole circumference view; (a) normal arrangement, (b) splitting gas sector, (c) splitting secondary-air sector, (d) spliting primary-air sector

inal flow rate. For example, the splitting ratio in the splitting gas sector design represents the ratio between the flow rate in the gas B sector, fig. 2(b) and the flow rate in the original gas sector, fig. 2(a).

Calculation method

Thermal performance calculation

The finite difference method (FDM) has been used in the design of RAPH by many manufacturers like Howden Global for a long time [11-16], but no shared code is available for free. Therefore, a program was developed by using a FDM to calculate the thermal performance of RAPH in our previous work [17]. The energy balance equation and the heat transfer equation can be expressed:

$$-\dot{m}c\frac{\partial t}{\partial Z}-\dot{M}C\frac{1}{r}\frac{\partial T}{\partial \theta}+\left[\lambda_Z\varphi_Z\frac{\partial^2 T}{\partial Z^2}+\lambda_\theta\varphi_\theta\frac{1}{r^2}\frac{\partial^2 T}{\partial \theta^2}+\lambda_r\varphi_r\frac{1}{r}\frac{\partial}{\partial r}\left(r\frac{\partial T}{\partial r}\right)\right]=0 \tag{1}$$

$$\dot{m}c\frac{\partial t}{\partial Z}=h\beta(T-t) \tag{2}$$

The heat transfer coefficient, *h*, can be calculated by Nusselt number:

$$\text{Nu}=\frac{hD_h}{\lambda} \tag{3}$$

The effectiveness of the RAPH is defined:

$$\varepsilon=\frac{t_{\text{g,in}}-t_{\text{g,out}}}{t_{\text{g,in}}-t_{\text{a,in}}} \tag{4}$$

In application, the outlet temperatures and pressure drops in the gas-, primary-air- and secondary-air-sectors are generally used to judge whether the performance of RAPH meets the demands of the boiler or not. Therefore, the accuracy of our program can be validated by comparing the calculation results of these parameters with the measured data in a coal-fired power plant. The temperature measurement grids are set at the inlet and the outlet of the RAPH. The temperatures of flue gas and air are measured and recorded per minute. We can obtain the measured data on the distributed control system when the boiler is operated under the design condition. As shown in tab. 3, the outlet temperatures of all fluid sectors calculated by the program agree fairly well with the measured results.

Table 3. The comparison between the calculation and the measurement

Outlet temperature	Calculation	Measurement	Relative deviation, [%]
$t_{\text{g,out}}$ [°C]	120.93	123.31	–1.93
$t_{\text{sec,out}}$ [°C]	372.65	370.27	0.64
$t_{\text{pri,out}}$ [°C]	362.69	359.38	0.92

Improved radian number

The original radian number [5] was proposed to characterize the ABS formation rate:

$$\text{Radian} = [SO_3][NH_3]([T_{ABS}] - [T_{rep}])$$

$$T_{rep} = 0.7\,T_{cold} + 0.3\,t_{g,exit} \tag{5}$$

where T_{ABS} is the initial formation temperature of ABS which can be calculation from the Muzio's study [18], T_{cold} – the temperature at cold end metal in RAPH, $t_{g,exit}$ – the outlet temperature of flue gas in RAPH, $[SO_3]$ and $[NH_3]$ – the volume concentrations of SO_3 and NH_3 in the flue gas, respectively. Since the radian number only depends on the concentration of SO_3 and NH_3, ABS initial formation temperature and the cold end metal temperature and outlet gas temperature.

However, for the RAPH with air bypass design or with some other flow designs, the temperature of cold end may not have a great change while that of the middle layer could change greatly compared with the normal RAPH. Therefore, the radian number computed from the temperatures of the cold end and exit gas is not reasonable to represent the ABS deposition problem. Moreover, the ABS deposition in the middle-layer is more difficult to clean due to the decay of the penetration of soot blowing device, which has received more attention of operators and designers. In this paper, an improved radian number is proposed:

$$Ra_{\text{impoved}} = R_{\text{axial}} + R_{\text{cir}}$$

$$\begin{cases} R_{\text{axial}} = \dfrac{T_{ABS} - T_{\text{cold bottom,ave}}}{T_{\text{cold top,ave}} - T_{\text{cold bottom,ave}}} \\ R_{\text{cir}} = \begin{cases} \dfrac{T_{ABS} - T_{\text{hot bottom,min}}}{T_{\text{hot bottom,ave}} - T_{\text{hot bottom,min}}} & \text{if} \quad T_{ABS,0} > T_{\text{hot bottom,min}} \\ 0 & \text{if} \quad T_{ABS,0} \le T_{\text{hot bottom,min}} \end{cases} \end{cases} \tag{6}$$

In eq. (6), $T_{\text{cold top,ave}}$ and $T_{\text{cold bottom,ave}}$ are the average temperatures at top and bottom boundaries of cold-layer matrix, respectively, $T_{\text{hot bottom,min}}$ and $T_{\text{hot bottom,ave}}$ – the minimum and average temperatures at bottom boundaries of hot-layer matrix, respectively, R_{axial} – the ratio of ABS deposition height to the total cold-layer height in axial direction, and R_{cir} – the ratio of ABS deposition angle range to the total range of gas section in the circumferential direction in the bottom of middle-layer. T_{ABS} is the formation temperature of ABS which can be calculated by the following equation [18].

$$P_{NH_3}(\text{atm})P_{SO_3}(\text{atm}) = 2.97 \cdot 10^{13} \exp\left(-\frac{54950}{\text{R}T}\right)$$

where R (= 1.987 cal/Kmol) is the universal gas constant, and T [K] – the flue gas temperature.

Compared to the original radian number, the improved radian number is a dimensionless number and can reflect the deposition in height and circumferential directions simultaneously. If Ra_{improved} is greater than 1, it means cross-layer ABS deposition occurs. The greater Ra_{improved} means that the ABS deposition is more serious and the plugging and corrosion problems induced by ABS would be more likely to happen and more difficult to solve.

Results and discussion

Effect of cold end protection

Figure 3 presents the matrix temperature profile along the axial direction in the conditions of inlet air heater mode and hot air re-circulation mode, respectively. As the inlet air temperature increases, the matrix temperature in the entire axial length gradually increases in either primary air heater mode or secondary air heater mode. In other words, the air heater mode can not only increase the average cold end temperature to alleviate the corrosion induced by sulfuric acid, but also help to increase the temperatures of intermedia-temperature matrix-layer and hot matrix-layer to alleviate the plugging and corrosion induced by ABS deposit. However, in the hot air re-circulation mode, with the increase of re-circulation rate, the cold end temperature increases but the temperature of medium and hot matrix-layer decrease. Therefore, the hot air re-circulation can only reduce the corrosion and foul induced by sulfuric acid in the cold matrix-layer, whereas it is not helpful to mitigate the plugging and corrosion induced by ABS in medium matrix-layer and would even aggravate the problem.

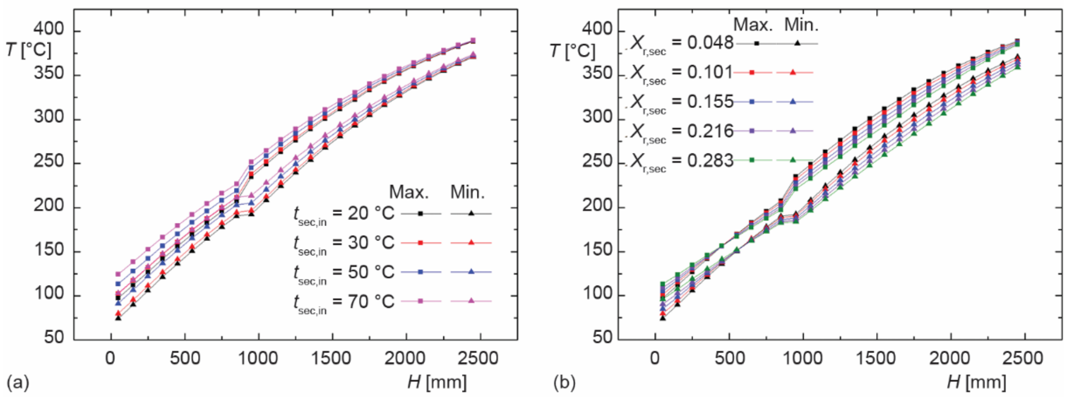

Figure 3 The matrix temperature profile along the axial direction at different re-circulation flow rate in: (a) secondary air heater mode, and (b) secondary air recirculation mode (*for color image see journal web site*)

Effects of air-flow bypass and splitting flow arrangements

Figure 4 shows the matrix temperature profile along the axial direction at different bypass rate. The matrix temperature increases in the entire height range with the increase of the secondary air bypass rate. As shown in fig. 8(b), the location of ABS deposition moves towards the cold end and the deposition range reduces gradually with the decrease in the efficiency as the increase in air bypass rate. Therefore, the air bypass is helpful to alleviate the plugging problem of RAPH, though it could decrease the efficiency of RAPH.

The matrix temperature and fluid temperature distributions of the RAPH in the splitting gas sector and splitting secondary-air sector arrangements are shown in figs. 5 and 6, respectively. As shown in fig. 5(a), in the gas-B sector, the cold end temperature of the matrix is increased much, while the temperature of the hot-layer and medium-layer starts to decline along the circumferential direction. By contrast, as shown in fig. 6(a), in the secondary-air-B

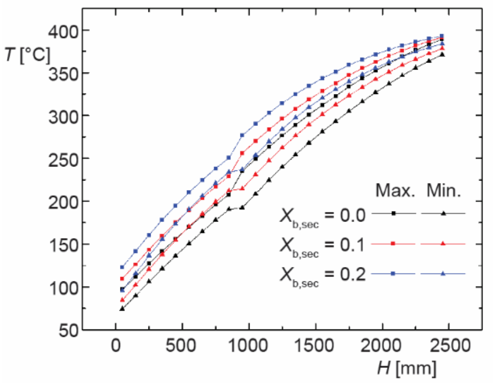

Figure 4 The maximum and minimum matrix temperature profile along the axial direction at different bypass rate (*for color image see journal web site*)

sector, the downward trend of matrix temperature is weakened in the cold- and medium--layers but intensified in the hot-layers especially in the hot end of the matrix along the circumferential direction.

The matrix temperature profiles along the axial length of RAPH in different arrangements are illustrated in fig. 7. For different arrangements, the trends of temperature profile with the splitting ratio are significantly different. As the increase in the splitting ratio, the trend of the profile curve becomes more and more concave in the splitting gas sector arrangement, fig. 7(a), whereas the trend of profile curve becomes more and more convex in the splitting air sector arrangements, fig. 7(b) and 7(c). In other words, the temperature of cold-layer is increased but that of medium and hot-layers is decreased in splitting gas sector arrangement. By contrast, the temperature of cold- and medium-layers is increased but that of hot-layer is

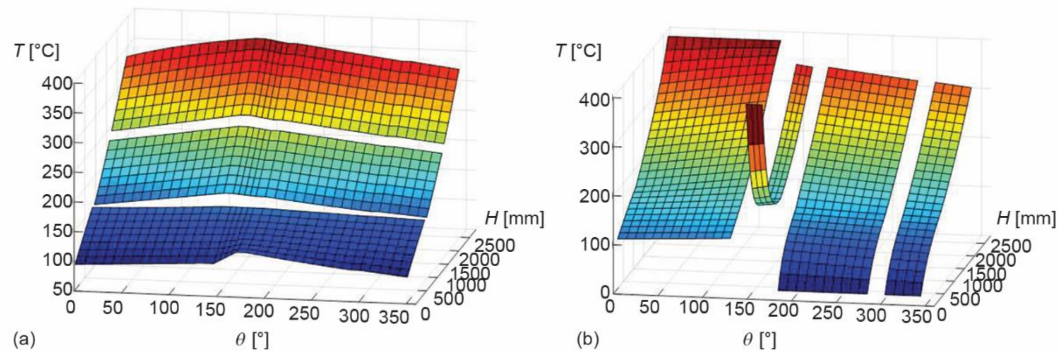

Figure 5. Matrix (a) and fluid (b) temperature distribution in splitting gas sector arrangement when $X_{c,g}$ = 0.15 (*for color image see journal web site*)

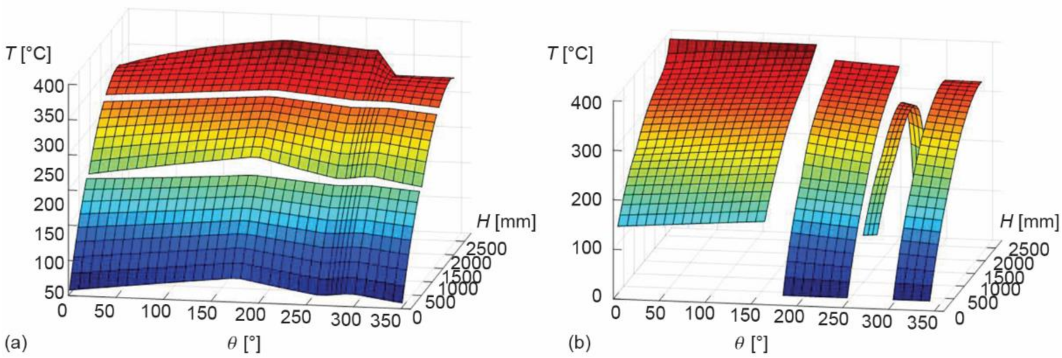

Figure 6. Matrix (a) and fluid (b) temperature distribution in splitting secondary air sector arrangement when $X_{c,sec}$ = 0.3 (*for color image see journal web site*)

decreased in splitting air sector arrangements. All these modified arrangements could increase the cold end temperature at the expense of the decrease in the effectiveness of RAPH. As shown in fig. 8(a), the cold end temperature increase with the decrease of the effectiveness of RAPH. It is clear that the splitting air sector arrangement is more efficient to increase the cold end temperature than the splitting gas sector arrangement and the air bypass arrangement.

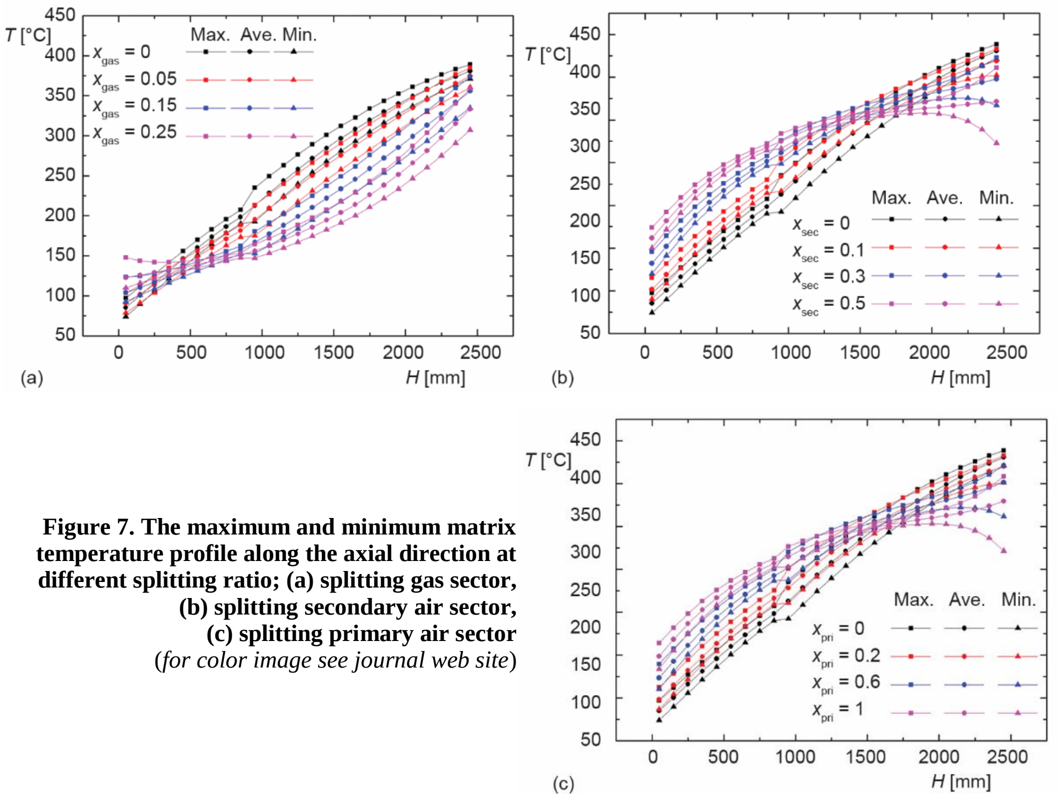

Figure 7. The maximum and minimum matrix temperature profile along the axial direction at different splitting ratio; (a) splitting gas sector, (b) splitting secondary air sector, (c) splitting primary air sector (*for color image see journal web site*)

Figure 8(b) presents the variation of height range of ABS deposition with the effectiveness of RAPH in different arrangements. The height range of ABS deposition gradually

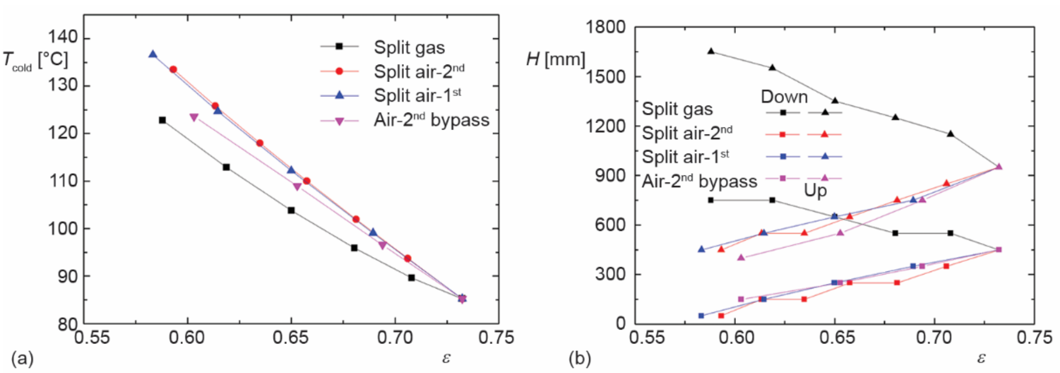

Figure 8. Average cold end temperature (a) and height range of ABS deposition (b) *vs.* effectiveness of RAPH in different flow arrangements (*for color image see journal web site*)

moves upwards in the splitting gas sector arrangement, which would lead to plugging induced by ABS deposition occur in medium matrix-layer. The height of ABS deposition gradually moves downwards in the splitting air sector arrangements, which could make the location of plugging induced by ABS move downwards and overlap with the ash deposition area induced by sulfuric acid condensation. Therefore, the total area of ash deposition would be augmented in splitting gas sector arrangement, which might lead to a more serious plugging, whereas it would be reduced in splitting air sector arrangements. From fig. 8(b), it is easy to find that the upper boundary of ABS deposition in RAPH with air bypass arrangement is lower than those in split sector arrangements, so air bypass is more efficient to reduce the ABS deposition in the middle-layer.

Comparative study of the improved- and original- radian number

As shown in fig. 9(a), for the RAPH using secondary air bypass, both the original radian number and the improved radian number decrease with the increase in the bypass rate of secondary air, which means that the ABS deposition can be greatly eased. In this case, both original and improved radian numbers can reflect the ABS deposition status. However, for the RAPH with air re-circulation, these two radian numbers have opposite trend with the re-circulation rate, as shown in fig. 9 (b). In this case, the original radian number gives a wrong estimation of ABS deposition status, since the ABS deposition range would become larger with the increase in air re-circulation rate, fig. 3. In fig. 9(c), the original radian number also give a wrong estimation for the RAPH with splitting gas arrangement, since the splitting gas arrangement could deteriorate the ABS deposition as previously analyzed. Moreover, the radian number for RAPH with air bypass arrangement is larger than the radian number for

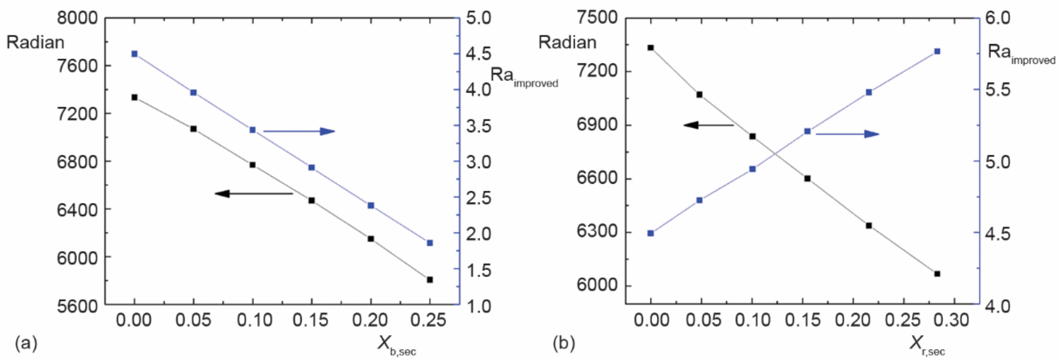

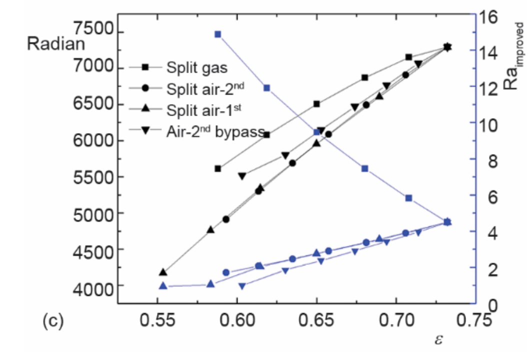

Figure 9. Comparison between original Radian number and improved Radian number; (a) *vs.* the bypass rate of secondary air, (b) *vs.* the re-circulation rate of secondary air, (c) *vs.* the effectiveness of RAPH for different splitting sector arrangement
(*for color image see journal web site*)

RAPH with splitting air arrangement. By contrast, the improved radian number Ra_{improved} for RAPH with air bypass arrangement is smaller than the cases with splitting air arrangement. Figure 8(b) has already shown that the air bypass is more efficient to ease the ABS deposition than other arrangements, so it means the improved radian number can give more accurate and reasonable estimation for ABS deposition than the original one.

Conclusions

In this paper, investigation has been conducted to figure out the characteristic of the temperature and ABS deposition distribution in different operating conditions or arrangements. The main findings can be summarized as follows.

- To increase the air bypass rate can increase the matrix temperature in the whole height range, and it is helpful to alleviate the plugging problem of RAPH. Moreover, the secondary air bypass is more effective than the splitting air sector arrangements.
- The inlet air heater mode is helpful to increase the overall temperature profile along axial length of RAPH. The hot air recirculation is not helpful to ease the plugging problem induced by ABS deposition in medium matrix layer and would even aggravate the problem.
- The splitting gas sector arrangement would cause more serious plugging problem. Whereas, the splitting air sector arrangements can alleviate the plugging induced by either sulfuric acid or ABS.
- The original radian number can only partially reflect the ABS deposition status, and in some cases, it would even give wrong estimation. An improved radian number is proposed which can give more accurate and reasonable estimation for ABS deposition status in the RAPH.

Acknowledgment

This work has been financially supported by the National Key R&D Program of China (2017YFB0602102).

Nomenclature

C – specific heat of matrix, [Jkg^{-1}K^{-1}]
c – specific heat of gas or air, [Jkg^{-1}K^{-1}]
D_h – hydraulic diameter, [mm]
H – height of the rotor, [mm], axial co-ordinate, [mm]
h – convective heat transfer coefficient, [Wm^{-2}K^{-1}]
$\dot{M}$ – mass flux of matrix, [kgs^{-1}]
$\dot{m}$ – mass flux of the fluid, [kgs^{-1}]
Nu – Nusselt number, [–]
Pr – Prandtl number, [–]
R – radius of the rotor, [m]
Ra_{improved} – improved radian number, [–]
Re – Reynolds number, [–]
r – radius co-ordinate, [mm]
T – matrix temperature, [°C]
T_{ABS} – formation temperature of ABS, [°C]
T_{cold} – average temperature of cold end, [°C]
$T_{\text{cold top,ave}}$ – average temperature at top boundary of cold layer matrix, [°C]
$T_{\text{cold bottom,ave}}$ – average temperature at bottom boundary of cold layer matrix, [°C]
$T_{\text{evaporation}}$ – evaporation temperature of ABS, [°C]
$T_{\text{hot bottom,min}}$ – minimum temperature at bottom boundary of hot layer matrix, [°C]
$T_{\text{hot bottom,ave}}$ – average temperature at bottom boundary of hot layer matrix, [°C]
T_{rep} – represented temperature, [°C]
t – gas or air temperature, [°C]
$t_{\text{g,exit}}$ – gas temperature at the outlet, [°C]
Z – axial co-ordinate, [mm]
[SO_3] – volume concentration of SO_3, [ppm]
[NH_3] – volume concentration of NH_3, [ppm]
X_b – bypass flow ratio ($=m_b/m_0$), [–]
$X_{b,\text{sec}}$ – bypass rate of secondary air flow
X_c – counter flow ratio ($=m_c/m_0$), [–]
X_r – re-circulation flow ratio ($=m_r/m_0$), [–]
$X_{r,\text{sec}}$ – re-circulation rate of secondary air flow

Greek symbols

β – heat-transfer surface area density of matrix, [m^{2}m^{-3}]
δ – trickness of the heat transfer plate, [mm]

ε – the effectiveness of RAPH
φ – fraction of solid of the matrix
λ – thermal conductivity, [$Wm^{-2}K^{-1}$]
θ – tangential co-ordinate or fluid sector angle, [°]
ρ – density, [kgm^{-3}]
Ω – rotational speed, [r per minute]

Subscripts

a – air
b – bypass flow
c – cold end or counter flow
g – gas
i – row number
in – inlet
j – column number
out – outlet
pri – primary air
sec – secondary air
r – re-circulation
0 – original flow rate

References

[1] Vuthaluru, H. B., French, D. H., Investigations into the Air Heater Ash Deposit Formation in Large Scale Pulverised Coal Fired Boiler, *Fuel*, *140* (2015), Jan., pp. 27-33
[2] Ruscio, A., *et al*., Comparison of Fine Ash Emissions Generated from Biomass and Coal Combustion and Valuation of Predictive Furnace Deposition Indices: A Review, *Journal of Energy Engineering*, *142* (2016), 2, p. E4015007
[3] Ma, Z., *et al*., Characteristics of NO_x Emission from Chinese Coal-Fired Power Plants Equipped with New Technologies, *Atmospheric Environment*, *131* (2016), Apr., pp. 164-170
[4] Shi, Y., *et al*., Formation and Decomposition of NH4HSO4 During Selective Catalytic Reduction of NO with NH_3 over V_2O_5-WO_3/TiO_2 Catalysts, *Fuel Processing Technology*, *150* (2016), Sep., pp. 141-147
[5] Burke, J., Johnson, K. L., Ammonium Sulfate and Bisulfate Formation in Air Preheaters, Technical Report PB-82-237025, Radian Corp., Austin, Tex., USA, 1982
[6] Menasha, J., *et al*., Ammonium Bisulfate Formation Temperature in a Bench-Scale Single-Channel Air Preheater, *Fuel*, *90* (2011), 7, pp. 2445-2453
[7] Chen, H., *et al*., Corrosion and Viscous Ash Deposition of a Rotary Air Preheater in a Coal-Fired Power Plant, *Applied Thermal Engineering*, *113* (2017), Feb., pp. 373-385
[8] Zhou, C., *et al*., Research Progress on Ammonium Bisulfate Formation and Control in the Process of Selective Catalytic Reduction, *Environmental Progress & Sustainable Energy*, *35* (2016), 6, pp. 1664-1672
[9] Chothani, C., Morey, R., Ammonium Bisulfate (ABS) Measurement for SCR NOx Control and Air Heater Protection, *MEGA* (2008), Paper 51, pp. 1-13
[10] Si, F., *et al*., Inferential Sensor for On-Line Monitoring of Ammonium Bisulfate Formation Temperature in Coal-Fired Power Plants, *Fuel Processing Technology*, *90* (2009), 1, pp. 56-66
[11] Bahnke, G., Howard, C., The Effect of Longitudinal Heat Conduction on Periodic-Flow Heat Exchanger Performance, *Journal of Engineering for Power*, *86* (1964), 2, pp. 105-117
[12] Skiepko, T., The Effect of Matrix Longitudinal Heat-Conduction on the Temperature-Fields in the Rotary Heat-Exchanger, *International Journal of Heat and Mass Transfer*, *31* (1988), 11, pp. 2227-2238
[13] Li, C. H., A Numerical Finite-Difference Method for Performance Evaluation of a Periodic-Flow Heat-Exchanger, *Journal of Heat Transfer-Transactions of the Asme*, *105* (1983), 3, pp. 611-617
[14] Wang, H., *et al*., Analysis on Thermal Stress Deformation of Rotary Air-Preheater in a Thermal Power Plant, *Korean Journal of Chemical Engineering*, *26* (2009), 3, pp. 833-839
[15] Nair, S., *et al*., Rotary Heat Exchanger Performance with Axial Heat Dispersion, *International Journal of Heat and Mass Transfer*, *41* (1998), 18, pp. 2857-2864
[16] Herraiz, L., *et al*., Reducing Water Usage with Rotary Regenerative Gas/Gas Heat Exchangers in Natural Gas-Fired Power Plants with Post-Combustion Carbon Capture, *Energy*, *90* (2015), Oct., pp. 1994-2005
[17] Wang, L., *et al*., Thermal Deformation Prediction Based on the Temperature Distribution of the Rotor in Rotary Air-Preheater, *Applied Thermal Engineering*, *90* (2015), Nov., pp. 478-488
[18] Muzio, L., *et al*., Ammonium Bisulfate Formation and Reduced Load SCR Operation, *Fuel*, *206* (2017), Oct., pp. 180-189

Paper submitted: May 24, 2018
Paper revised: July 16, 2018
Paper accepted: July 16, 2018